Optimal compression and energy confinement of optical Airy bullets

DOMENICO BONGIOVANNI[1], BENJAMIN WETZEL[1,2*], YI HU[3], ZHIGANG CHEN[3,4] AND ROBERTO MORANDOTTI[1,5*]

[1]INRS-EMT, 1650 Blvd. Lionel-Boulet, Varennes, Québec J3X 1S2, Canada
[2]School of Mathematical and Physical Sciences, University of Sussex, Sussex House, Falmer, Brighton BN1 9RH, UK
[3]The MOE Key Laboratory of Weak-Light Nonlinear Photonics, TEDA Applied Physics Institute and School of Physics, Nankai University, Tianjin 300457, China
[4]Department of Physics & Astronomy, San Francisco State University, San Francisco, CA 94132, USA
[5]Institute of Fundamental and Frontier Sciences, University of Electronic Science and Technology of China, Chengdu 610054, China
[6]National Research University of Information Technologies, Mechanics and Optics, St. Petersburg, Russia
**benjamin.wetzel@emt.inrs.ca, *morandotti@emt.inrs.ca*

Abstract: We report on an approach to generate non-diffractive and non-dispersive Airy[3] bullets with enhanced spatio-temporal energy confinement. By appropriately reshaping the initial spectral components in the Fourier domain, the resulting optical bullets show a significant enhancement of their central lobe intensity while exhibiting a reduced spatio-temporal outspread of the surrounding sub-lobes - typical of Airy[3] bullets. Numerically, we demonstrate that when propagating in dispersive media within a linear regime, such optimized Airy[3] bullets maintain the peculiar properties of their "standard" counterparts, including curved trajectories, non-spreading features and self-healing. We foresee direct applications in novel and non-disruptive optical techniques for imaging, tomography and spatio-temporally resolved spectroscopy.

References and links

1. Y. Silberberg, "Collapse of optical pulses," Opt. Lett. **15**, 1282-1284 (1990).
2. A. M. Boris, M. Dumitru, W. Frank, and T. Lluis, "Spatiotemporal optical solitons," J. Opt. B. **7**, R53 (2005).
3. P. Di Trapani, G. Valiulis, A. Piskarskas, O. Jedrkiewicz, J. Trull, C. Conti, and S. Trillo, "Spontaneously generated X-shaped light bullets," Phys. Rev. Lett. **91**, 093904 (2003).
4. M. A. Porras and P. Di Trapani, "Localized and stationary light wave modes in dispersive media," Phys. Rev. E **69**, 066606 (2004).
5. Y. S. Kivshar and G. Agrawal, "Optical solitons: from fibers to photonic crystals," (Academic press, 2003).
6. A. Chong, W. H. Renninger, D. N. Christodoulides, and F. W. Wise, "Airy-Bessel wave packets as versatile linear light bullets," Nature Photon. **4**, 103-106 (2010).
7. D. Abdollahpour, S. Suntsov, D. G. Papazoglou, and S. Tzortzakis, "Spatiotemporal Airy light bullets in the linear and nonlinear regimes," Phys. Rev. Lett. **105**, 253901 (2010).
8. M. V. Berry and N. L. Balazs, "Nonspreading wave packets," Am. J. Phys. **47**, 264-267 (1979).
9. G. A. Siviloglou and D. N. Christodoulides, "Accelerating finite energy Airy beams," Opt. Lett. **32**, 979-981 (2007).
10. G. A. Siviloglou, J. Broky, A. Dogariu, and D. N. Christodoulides, "Observation of accelerating Airy beams," Phys. Rev. Lett. **99**, 213901 (2007).
11. P. Saari, "Laterally accelerating Airy pulses," Opt. Express **16**, 10303-10308 (2008).
12. J. Broky, G. A. Siviloglou, A. Dogariu, and D. N. Christodoulides, "Self-healing properties of optical Airy beams," Opt. Express **16**, 12880 (2008).
13. P. Polynkin, M. Kolesik, J. V. Moloney, G. A. Siviloglou, and D. N. Christodoulides, "Curved plasma channel generation using ultraintense Airy beams," Science **324**, 229-232 (2009).
14. N. Voloch-Bloch, Yossi Lereah, Y. Lilach, A. Gover, and A. Arie, "Generation of electron Airy beams," Nature **494**, 331-335 (2013).
15. J. Baumgartl, M. Mazilu, and K. Dholakia, "Optically mediated particle clearing using Airy wavepackets," Nature Photon. **2**, 675-678 (2008).

16. N. Wiersma, N. Marsal, M. Sciamanna, and D. Wolfersberger, "All-optical interconnects using Airy beams," Opt. Lett. **39**, 5997-6000 (2014).
17. M. Clerici, Y. Hu, P. Lassonde, C. Milián, A. Couairon, D. N. Christodoulides, Z. Chen, L. Razzari, F. Vidal, F. Légaré, D. Faccio, and R. Morandotti, "Laser-assisted guiding of electric discharges around objects," Science Advances **1**, e1400111 (2015).
18. T. Vettenburg, H. I. Dalgarno, J. Nylk, C. Coll-Lladó, D. E. Ferrier, T. Čižmár, F. J. Gunn-Moore, and K. Dholakia, "Light-sheet microscopy using an Airy beam," Nat. Methods **11**, 541-544 (2014).
19. I. M. Besieris and A. M. Shaarawi, "A note on an accelerating finite energy Airy beam," Opt. Lett. **32**, 2447-2449 (2007).
20. A. Mathis, F. Courvoisier, L. Froehly, L. Furfaro, M. Jacquot, P. A. Lacourt, and J. M. Dudley, "Micromachining along a curve: Femtosecond laser micromachining of curved profiles in diamond and silicon using accelerating beams," Appl. Phys. Lett. **101**, 071110 (2012).
21. P. Polynkin, M. Kolesik, and J. Moloney, "Filamentation of femtosecond laser Airy beams in water," Phys. Rev. Lett. **103**, 123902 (2009).
22. W.-P. Zhong, M. R. Belić, and T. Huang, "Three-dimensional finite-energy Airy self-accelerating parabolic-cylinder light bullets," Phys. Rev. A **88**, 033824 (2013).
23. F. Deng and D. Deng, "Three-dimensional localized Airy-Hermite-Gaussian and Airy-Helical-Hermite-Gaussian wave packets in free space," Opt. Express **24**, 5478-5486 (2016).
24. W.-P. Zhong, M. R. Belić, and Y. Zhang, "Airy-Tricomi-Gaussian compressed light bullets," Eur. Phys. J. Plus **131**, 1-8 (2016).
25. J. Sharpe, U. Ahlgren, P. Perry, B. Hill, A. Ross, J. Hecksher-Sørensen, R. Baldock, and D. Davidson, "Optical projection tomography as a tool for 3D microscopy and gene expression studies," Science **296**, 541-545 (2002).
26. J. G. Fujimoto, "Optical coherence tomography for ultrahigh resolution in vivo imaging," Nat. Biotechnol. **21**, 1361-1367 (2003).
27. J. A. Davis, M. J. Mitry, M. A. Bandres, and D. M. Cottrell, "Observation of accelerating parabolic beams," Opt. Express **16**, 12866-12871 (2008).
28. M. A. Bandres, "Accelerating parabolic beams," Opt. Lett. **33**, 1678-1680 (2008).
29. B. K. Singh, R. Remez, Y. Tsur, and A. Arie, "Super-Airy beam: self-accelerating beam with intensified main lobe," Opt. Lett. **40**, 4703-4706 (2015).
30. D. Bongiovanni, Y. Hu, B. Wetzel, R. A. Robles, G. Mendoza González, E. A. Marti-Panameño, Z. Chen, and R. Morandotti, "Efficient optical energy harvesting in self-accelerating beams," Sci. Rep. **5**, 13197 (2015).
31. Y. Hu, D. Bongiovanni, Z. Chen, and R. Morandotti, "Multipath multicomponent self-accelerating beams through spectrum-engineered position mapping," Phys. Rev. A **88**, 043809 (2013).
32. O. Vallée and M. Soares, "Airy functions and applications to physics," (Imperial College Press, 2004).
33. G. A. Siviloglou, J. Broky, A. Dogariu, and D. N. Christodoulides, "Ballistic dynamics of Airy beams," Opt. Lett. 33, 207-209 (2008).
34. A.M. Weiner, "Femtosecond pulse shaping using spatial light modulators," Rev. Sci. Instrum. **71**, 1929-1960 (2000).
35. Y. Hu, M. Li, D. Bongiovanni, M. Clerici, J. Yao, Z. Chen, J. Azaña, and R. Morandotti, "Spectrum to distance mapping via nonlinear Airy pulses," Opt. Lett. **38**, 380-382 (2013).
36. S. Akturk, X. Gu, P. Gabolde and R. Trebino, "The general theory of first-order spatio-temporal distortions of Gaussian pulses and beams," Opt. Express **13**, 8642-8661 (2005).
37. M. Dallaire, N. McCarthy and M. Piché, "Spatiotemporal Bessel beams: theory and experiments," Opt. Express **17**, 18148-18164 (2009).
38. P. Piksarv, A. Valdmann, H. Valtna-Lukner and P. Saari, "Ultrabroadband Airy light bullets," Laser Phys. **24**, 085301 (2014).

1. Introduction

When propagating in a homogenous dielectric medium, an optical wave packet naturally tends to spread in both space and time due to the combined effects of diffraction and dispersion. Over the past decade, tremendous efforts have been made by the community to suppress this energy spreading through the generation of so-called “optical light bullets” [1-4]. Optical nonlinearities are able to compensate dispersion/diffraction, thus allowing to maintain the temporal/spatial shape of an optical pulse/beam throughout propagation, commonly referred to as temporal/spatial solitons [5]. Although of high interest for numerous applications, the use of nonlinearity to mitigate such spreading is limited by particular combinations of propagation media and optical wave packet parameters (i.e. beam waist, pulse duration, power), which not only needs to be perfectly characterized, but also cannot be

easily tuned over a wide range of parameters. Additionally, the associated optical bullets, basically in need of intense powers to gain nonlinearity, may be incompatible with non-disruptive or non-invasive techniques including, for example, biomedical imaging or optical probing, where the samples are prone to be damaged under intense light illumination. In the linear regime, non-diffractive and non-dispersive solutions can be employed to produce optical bullets by means of X-wave or O-wave optical structures [3,4]. Quite recently, self-accelerating solutions (namely Airy beams/pulses) have offered the opportunity to generate linear optical bullets with new features [6,7]. Such characteristics [8-21] have indeed proven to be useful in numerous applications and in several fields including, among others, the generation of curved plasma channels [13], photo-induced waveguides [16], curved electric discharges [17], as well as for optical trapping [15], optical micro/nano-processing [20], and light-sheet microscopy [18].The associated method for the generation of Airy bullets is straightforward, since the Airy wave packet can exist in one dimension and can be hence directly applied to shape the temporal profile of optical bullets, while in the spatial domain, one can adopt non-diffractive beams to generate different optical bullets, such as Airy-Bessel [6], Airy-Airy (i.e. Airy^3) [7], Airy-Parabolic-Cylinder [22], Airy-Hermite-Gaussian [23] and Airy-Tricomi-Gaussian [24] . Among others, Airy^3 bullets are of particular interest as they can accelerate in both the spatial and temporal domains. However, such bullets have the intrinsic disadvantage of occupying a large (spatio-temporal) volume filled by numerous sub-lobes, while only the (intense) main lobe is in fact relevant for most applications [13,15,16,18,20,21]. This drawback is thus expected to strongly restrict the range of targeted applications, especially in areas where low energies and yet high confinement of the bullets are simultaneously required, including for example spatio-temporally resolved and non-disruptive optical probing, microscopy, as well as biomedical applications [18,25,26]. To the best of our knowledge, few studies have addressed the possibility of reshaping these bullets to reach an optimization of the energy distribution while still maintaining their useful properties [27-31].

In this paper, we report numerical investigations related to the optimization of an Airy^3 bullet. In particular, a method is provided to generate an energy-confined light pulse by reshaping both the temporal and spatial spectra of the conventional Airy^3 bullet. We show that an appropriate compression of the spatiotemporal input spectrum leads to the generation of a "narrow" version of the conventional light localization, which exhibits a significant enhancement in terms of peak intensity. Furthermore, such an increase is matched by the confinement of its spatio-temporal profile, while still preserving its peculiar propagation characteristics (i.e. acceleration and self-healing properties).

2. Theory of (3+1)D accelerating optical bullets

In the linear regime, the spatio-temporal propagation of an optical pulse in a dispersive medium can be described by the (3+1) D paraxial differential equation:

$$i\frac{\partial\phi\left(\vec{r},\tau\right)}{\partial z}+\frac{1}{2\beta\left(\omega_0\right)}\nabla_{\perp}^{2}\phi\left(\vec{r},\tau\right)=\frac{\beta_2\left(\omega_0\right)}{2}\frac{\partial^2\phi\left(\vec{r},\tau\right)}{\partial\tau^2}, \qquad (1)$$

where $\phi(\vec{r},\tau)=\phi(x,y,z,\tau)$ is the slowly-varying envelope of the electric field, x and y are the transverse coordinates, z refers to the longitudinal propagation distance, and $\tau=t-z/v_g$ represents the time coordinate in a frame moving with the group velocity v_g. The transverse Laplacian operator $\nabla_{\perp}^{2}=\partial^2/\partial x^2+\partial^2/\partial y^2$ in Eq. (1) describes the diffraction effect, while the right hand side term accounts for dispersion, where the wave number $\beta(\omega_0)=\omega_0 n(\omega_0)/c$ and group velocity dispersion $\beta_2(\omega_0)=\partial^2\beta/\partial\omega^2\,|_{\omega_0}$ are evaluated at the carrier frequency ω_0.

Using the dimensionless coordinates $(\vec{R},Z)=(X,Y,T,Z)=(x/w_0,y/w_0,\tau/\tau_0,z/L_{diff})$, where w_0 is the beam spatial width and τ_0 the pulse duration, Eq. (1) can be recast into a normalized form by introducing the diffraction length $L_{diff}=\beta(\omega_0)w_0^{\,2}$ and dispersion length $L_{disp}=\tau_0^{\,2}/|\beta_2(\omega_0)|$:

$$i\frac{\partial\phi\left(\vec{R},Z\right)}{\partial Z}+\frac{1}{2}\left[\frac{\partial^2\phi\left(\vec{R},Z\right)}{\partial X^2}+\frac{\partial^2\phi\left(\vec{R},Z\right)}{\partial Y^2}-sign\left[\beta_2\right]\frac{L_{diff}}{L_{disp}}\frac{\partial^2\phi\left(\vec{R},Z\right)}{\partial T^2}\right]=0, \qquad (2)$$

Here, we consider the propagation in an anomalous dispersion regime ($\beta_2<0$). As both the spatial and temporal coordinates can be readily rescaled in this expression, we here assume that dispersion and diffraction have the same quantitative effect along propagation so that $L_{diff}=L_{disp}$. In this case, the spatiotemporal evolution of an optical bullet is isotropic and can be simplified for analytic purposes, yielding:

$$i\frac{\partial\phi\left(\vec{R},Z\right)}{\partial Z}+\frac{1}{2}\nabla^2\phi\left(\vec{R},Z\right)=0, \qquad (3)$$

where $\nabla^2=\partial^2/\partial X^2+\partial^2/\partial Y^2+\partial^2/\partial T^2$ is the spatiotemporal Laplacian operator.

3. Finite-energy Airy[3] bullet

In what follows, we consider an Airy[3] bullet [7,9] whose initial amplitude takes the form of $\phi(\vec{R},0)\approx Ai(X)Ai(Y)Ai(T)e^{(\alpha_X X+\alpha_Y Y+\alpha_T T)}$, where *Ai* refers to the Airy function [32] and the truncation coefficients $\alpha_i<<1\ (i=X,Y,T)$ are positive and constants (i.e. in relation with the finite energy of the Airy[3] bullet). In the Fourier space, the corresponding spatio-temporal spectrum is characterized by a 3D cubic spectral phase $\Phi(\vec{K},0)=e^{i\rho(\vec{K})}\,e^{-\left(\alpha_X k_X^{\,2}+\alpha_Y k_Y^{\,2}+\alpha_T k_T^{\,2}\right)}$, yielding a solution to Eq. (3) of the form:

$$\begin{aligned}\phi\left(\vec{R},Z\right)=\ & Ai\left[X-\frac{Z^2}{4}+i\alpha Z+\alpha^2\right]Ai\left[Y-\frac{Z^2}{4}+i\alpha Z+\alpha^2\right]Ai\left[T-\frac{Z^2}{4}+i\alpha Z+\alpha^2\right]\\ & \exp\left[\alpha\left(2\alpha^2+X+Y+T-\frac{3}{2}Z^2\right)\right]\exp\left[i\left(X+Y+T+6\alpha^2-\frac{Z^2}{2}\right)\frac{Z}{2}\right]\end{aligned} \qquad (4)$$

An ideal Airy[3] bullet moves freely along the parabolic trajectory defined as $(X,Y,T)=(Z^2/4,Z^2/4,Z^2/4)$, for which the bullet intensity profile remains invariant over the longitudinal propagation (i.e. non-diffractive and non-dispersive).

In the dimensionless space (X,Y,T), the largest value of the beam intensity evolves along the parabolic trajectory $(Z^2/4,Z^2/4,Z)$, while the temporal shift of the peak power in the longitudinal direction exhibits the trajectory $T=Z^2/4$, which physically corresponds to a modification in the propagation velocity of the Airy wave packet. Note that, for the sake of simplicity, the truncation parameters of each component in Eq. (4) are assumed equal, so that $\alpha=\alpha_X=\alpha_Y=\alpha_T$. In our simulations, we considered a small truncation factor of $\alpha=0.04$ in order to obtain a bullet that can preserve its shape over a sufficient propagation distance, while at the same time ensuring that the numerical grid span is sufficiently discretized. This

was necessary to both encompass properly the whole bullet and resolve accurately the fine bullet characteristics (taking into account the computational memory limitation of our system).

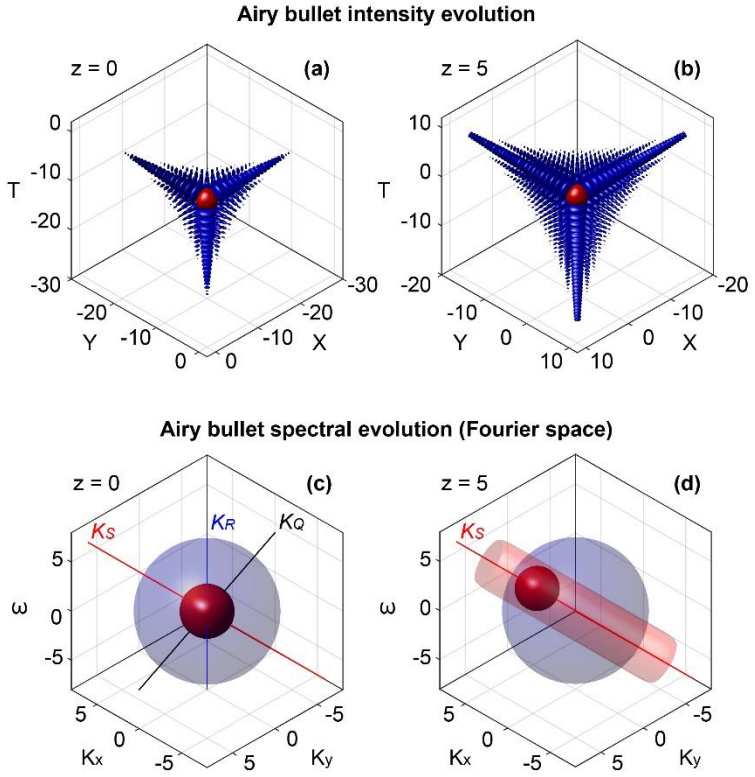

Fig. 1. (a,b) Spatio-temporal and (c,d) spectral intensity isosurfaces (blue shading) of a (finite-energy) Airy[3] bullet at $Z = 0$ and $Z = 5$, respectively. Red isosurfaces (95% intensity cutoff) highlight the bullet main lobe in (a,b), and its spectral counterpart in (c,d). The red line in (c,d) corresponds to the central axis of the red shaded cylinder in (d), i.e. the channel containing the spectral components of the main lobe during bullet propagation.

Figure 1 shows the intensity profile of the Airy[3] bullet and its Fourier space counterpart (95% cutoff isosurfaces) at two different propagation distances (i.e., $Z = 0$ and $Z = 5$). As shown in Fig. 1(a,b), the spatio-temporal wave packet is characterized by an intense main lobe (highlighted in red), as well as numerous sub-lobes. Although one may identify non negligible spreading when approaching $Z = 5$ (i.e. the increase of the bullet expansion due to its finite energy), we verified that the main lobe maintains its shape over a significant propagation range and follows closely the predicted parabolic trajectory along the direction $\vec{S} = (X, Y, T) = (Z^2/4, Z^2/4, Z^2/4)$.

In the Fourier space, the intensity isosurfaces shown in Fig. 1(c,d) exhibit a spherical shape (blue isosurface), intrinsically associated to the spherical symmetry set by the 3D Gaussian amplitude of the input spectrum. In contrast, the spectral content associated with the bullet main lobe (smaller red isosurface) changes along propagation [Fig. 1(c,d)]. In particular, the main lobe spectral content is confined within an elliptic cylinder (red shading). Such cylinder is orientated along the axis $\vec{K}_S$ with the half-axes defined along the

(orthogonal) directions $\vec{K}_Q = (K_X, -K_Y, 0)$ and $\vec{K}_R = (-K_X, -K_Y, 2\omega)$. This indicates that part of the energy does not contribute to the main lobe and is typically wasted for most applications based only on the accelerating properties of the main lobe.

4. Compressed Airy[3] Bullet

The fact that the spectral components associated with the main lobe of Airy[3] bullets are found within a specific spectral location is important for optimizing the bullet characteristics, as targeted in our current work. Indeed, by properly reshaping its spectral content, we can obtain a significant enhancement of the bullet main lobe intensity together with reduced overall spatiotemporal expansion. This can be achieved by squeezing the initial spherical spectrum of the Airy[3] bullet into the ellipsoid associated with the bullet main lobe (in a similar way to the approach already reported in the spatial domain only for two-dimensional Airy beams [30]), i.e., by compressing the spatio-temporal spectral intensity along both the directions $\vec{K}_Q = (K_X, -K_Y, 0)$ and $\vec{K}_R = (-K_X, -K_Y, 2\omega)$. We define the compression parameters as the ratio between the Gaussian waist α_Q (or α_R) obtained after the spectral compression along $\vec{K}_Q$ (or $\vec{K}_R$) and the initial waist of the spectrum α given in Eq.(4), so that $C_Q = \alpha_Q / \alpha$, and $C_R = \alpha_R / \alpha$.

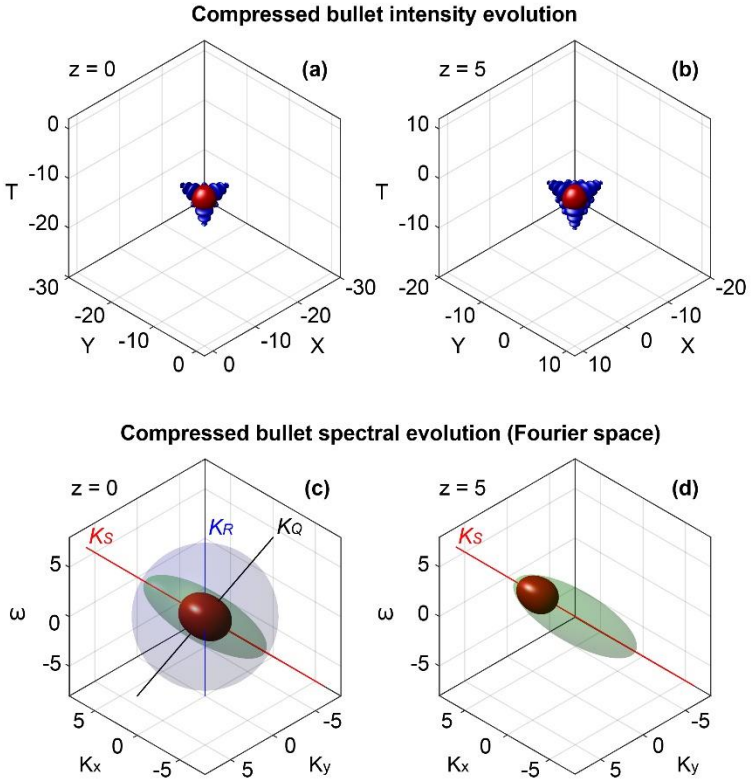

Fig. 2. Isosurfaces plots of the bullet generated using a "squeezed" spectrum along $\vec{K}_Q$ and $\vec{K}_R$ with a compression factor $C_Q = C_R = 8$. The initial spectrum (blue sphere) shown in (c),

corresponding to the classic Airy[3] bullet, is reshaped into an ellipsoid (green shading). Details are as those reported in the caption of Fig. 1.

In Fig. 2, we show numerical results obtained by first employing a symmetric compression (i.e. $C_Q = C_R = 8$ in this example) of the spherical spectrum in Fig. 1. The compressed spectrum is depicted as green isosurfaces, and compared with the initial Gaussian spectrum (blue shading). Accordingly, the spatiotemporal profile of the bullet (blue) exhibits a reduced expansion compared to the classic case, but the shape of the main lobe (red) remains almost unaffected at both propagation distances [Fig. 2(a,b)]. Note that in the following, we consider only a reshaping (i.e. redistribution) of the initial bullet spectral intensity so that, for any compression factor used, the total bullet energy remains constant and equal to unity.

5. Impact of Airy[3] bullet compression

In the following, we compare the classic bullet of Fig. 1 with the newly generated bullet of Fig. 2, and summarize the corresponding results in Fig. 3.

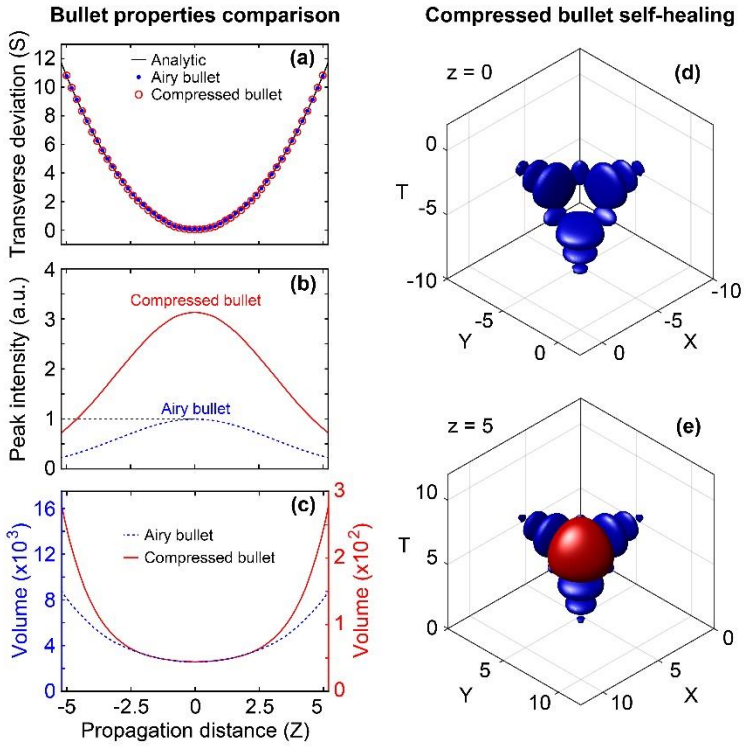

Fig. 3. Comparison of (a) spatiotemporal trajectories, (b) peak intensities and (c) comparison of the volumes along propagation between a compressed bullet and a classic Airy bullet. (d-e) Illustration of the self-healing behavior for the newly generated bullet in Fig. 2. The main lobe of the bullet is removed at $Z = 0$ in (d), and regenerated at $Z = 5$ in (e).

As seen in Fig. 3(a), the compressed bullet (red circles) maintains the same trajectory as for its uncompressed counterpart (blue dots) to follow the predicted parabolic path over the range $Z = [-5:5]$ (black line in Fig. 3(a)]. Yet, remarkably, it exhibits a significant

enhancement (i.e. by a factor > 3) of the peak intensity in comparison with its classic equivalent (and whose maximal peak intensity is used for normalization [Fig. 3(b)]). What is probably the most striking feature is illustrated in Fig. 3(c), where we extracted and compared the volume of the bullet in both the "classic" and compressed cases. Such volumes are calculated as the sum of the overall spatio-temporal span ($V = \Delta X.\Delta Y.\Delta T$) where the bullet intensity is above 0.1% of its peak intensity, and are further normalized with respect to the value for the main lobe of the Airy[3] bullet shown in Fig. 1(a). One can notice the drastic volume reduction of the compressed bullet - up to two orders of magnitude (see left/right axis scale) when compared to the classic case. In order to verify that the newly generated bullet still exhibits the features of standard Airy beams, we investigate its self-healing properties. In a typical example, its main lobe is numerically removed at $Z = 0$ [Fig. 3(d)]. As for a conventional Airy beam, the main lobe is regenerated during propagation [Fig. 3(e)]. Therefore, the bullet can be optimized in terms of intensity and spatio-temporal expansion, while maintaining its properties via a proper spectral compression, which could not be reached otherwise (e.g. by only using a Gaussian shape with a higher truncation parameter).

In what follows, we report a more detailed and quantitative study of the impact of the spectral compression on the bullet properties at $Z = 0$.

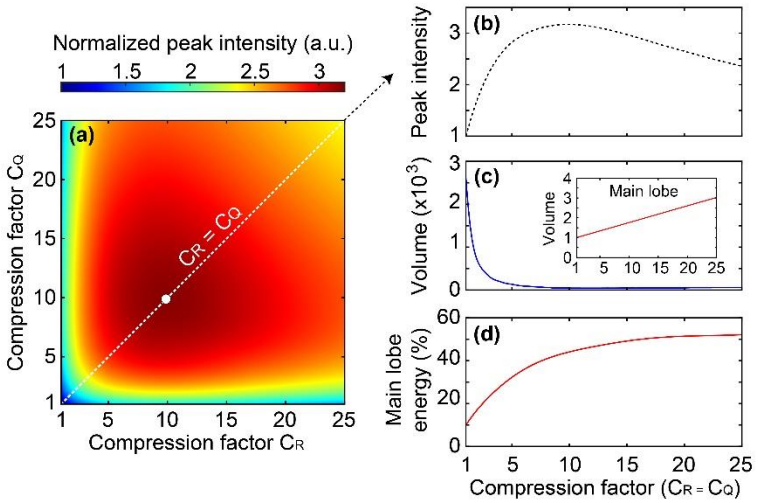

Fig. 4. (a) Peak intensity at $Z = 0$ as a function of the spectral compression factors C_Q and C_R (the optimal value is shown with a white dot). (b) Peak intensity and (c) volume of the bullet for symmetric compression (i.e. along the white dashed line in (a), where $C_Q = C_R$). The inset in (c) illustrates the volume of the main lobe upon spectral compression. (d) Corresponding energy ratio associated to the main lobe.

The truncation factor is the same as in Figs. 1-3, i.e. $\alpha = 0.04$. Figure 4(a) shows a colorplot of the peak intensity as a function of both compression factors C_Q and C_R. One can readily see that a significant intensity enhancement can be obtained even for low compression factors, and that an optimal value tends to appear for symmetric compression, i.e., $C_Q = C_R$. Under this condition (white dashed diagonal line), the relevant bullet properties are extracted and illustrated in Figs. 4(b-d). The maximum peak intensity enhancement appears for compression factors around 10. Deviations from this value lead to a squeezed spectrum that does not overlap perfectly with the spectral components associated to the main lobe, and

hence cause the peak intensity to decrease [Fig. 4(b)]. The impact of spectral compression on the overall bullet volume is shown in Fig. 4(c), where one can observe an exponential-like decay of the volume as the bullet spectrum is compressed, until reaching quasi-saturation for compression greater than ~10. In contrast, the bullet main lobe volume varies quite slowly and exhibits a linear increase with the degree of squeezing [see the inset in Fig. 4(c)]. Therefore, we can infer that the energy stored in the main lobe increases monotonically with the compression factor, as further illustrated in Fig. 4(d). The main lobe contains only about 10% of the total bullet energy for the classic "noncompressed" Airy[3] bullet, while for the compressed bullet of Fig. 2 (i.e. $C_Q = C_R = 8$), this ratio reaches more than 40%, i.e. a 4-fold increase. In addition, our numerical results predict the possibility to concentrate more than half of the bullet energy in the main lobe for a compression factor of $C_Q = C_R \approx 10$.

Our approach presents two advantages: not only it increases the intensity/energy of the bullet main lobe, but it also reduces its overall spatio-temporal expansion. Clearly, both aspects are associated with an improvement of the bullet energy confinement (here calculated as the ratio between energy and volume), as illustrated in Fig. 5.

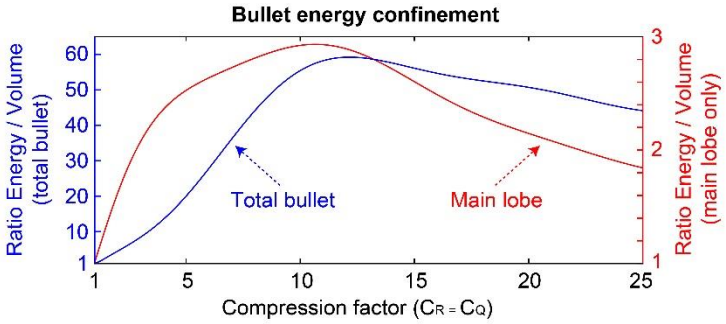

Fig. 5. Energy confinement of the total bullet (blue line) and its main lobe (red line) as a function of spectral compression. The energy confinement is calculated as the average ratio between energy and volume shown in Fig. 4(c-d), and normalized to unity with respect to the case of an uncompressed Airy[3] bullet.

We can thus observe that the energy confinement of the bullet main lobe (red line) is indeed enhanced by a factor of approximately 3 for an optimal compression factor of around 10. The main significant aspect of such compression is nevertheless associated with the overall bullet energy confinement, which can be improved by a factor of as much as 50 for a similar degree of spectral compression.

6. Discussion

The impact of spectral compression depends clearly on the initial truncation parameter. Here we focused on the case of $\alpha = 0.04$ (due to numerical grid limitations) that mimics typical experimental truncation values [10,12,33]. We conducted additional numerical simulations for lower values of α - generally used to increase the distance for which Airy beams are non-spreading. In such cases, our proposed method provides an even more efficient way to improve the bullet energy confinement, yielding, e.g., to a bullet energy confinement enhanced by a factor of 150 for a truncation factor $\alpha = 0.02$.

Although out of the scope of this study, we foresee that several experimental implementations of an Airy[3] bullet spectral reshaping could be readily obtained. In fact, it is worth noting that the potential energy confinement reported here is intrinsically associated

with an optimal overlap of the overall spectral components with the spectral location of the bullet main lobe (i.e. the red shaded section shown in Fig. 1(d)). In this framework, we expect that similar features can be observed by redistributing the bullet spectral content in an appropriate manner before applying, in the Fourier plane, i) a cubic phase for the temporal shaping [34, 35] (along ω, to generate an Airy pulse), ii) a "spatial" cubic phase [10,13,14] (with a 2D spatial light modulator - SLM) - following a proper spatial compression, as well as iii) angular dispersion and iv) a front tilt, in order to ensure the desired projection of the bullet spectrum onto the $[K_X, K_Y]$ plane of the spatial SLM [36]. The actual implementation is expected to require additional adjustments that will be the subject of further investigation, taking into account the numerical apertures and physical parameters of the system. Nevertheless, we believe that such an approach may be implemented through the conjoint use of widely available dispersive and focusing optical elements such as gratings and lenses, along with spatial light modulators ensuring the imprinting of the desired spectral phase on both the (distinct) spatial and temporal components, i.e. as in a 3D expansion of already realized spatial and temporal waveshaping implementations [6,7,30,37,38].

In this framework, it is worth underlining that the compressed Airy^3 bullets studied here possess, for each propagation distance, the peculiar property of presenting a reduced and limited spectral bandwidth compared to its "classic" counterpart. We therefore expect these peculiar bullets to open new avenues to applications such as spatio-temporally resolved spectroscopy, where resolution could be greatly enhanced.

7. Conclusion

We reported a numerical study showing the ability to realize spatiotemporal energy confinement of an Airy^3 bullet by way of an appropriate spectral reshaping of the bullet amplitude in the Fourier space. The spectral compression proposed here has the potential to "squeeze" a classic Airy^3 bullet, and can hence lead to an enhanced energy confinement, while the newly generated bullet maintains the peculiar properties of standard Airy bullets, including self-acceleration, diffraction/dispersion-less propagation and self-healing. We expect these results to have a significant impact for optimizing accelerating optical bullets in applications requiring non-disruptive and non-invasive techniques, including for example biomedical imaging, highly localized optical probing, and spatio-temporally resolved spectroscopy.

8. Funding and Acknowledgements

This work was supported by MERST Quebec and the NSERC (Natural Sciences and Engineering Research Council of Canada), and by the US National Science Foundation and Army Research Office. D.B. gratefully thanks the funding received from a Plasma Québec Fellowship. B.W. acknowledges the support from the People Programme (Marie Curie Actions) of the European Union's FP7 Programme under REA grant agreement INCIPIT (PIOF-GA-2013-625466). Y.H. acknowledges the support of the National Natural Science Foundation of China (NSFC) (11504186, 61575098) and 111 Project in China (B07013).